

Hydrogen transfer in photoexcited phenol/ammonia clusters by UV–IR–UV ion dip spectroscopy and *ab initio* molecular orbital calculations.

I. Electronic transitions

Shun-ichi Ishiuchi

Department of Chemistry, Faculty of Science and Technology, Keio University, 3-12-1 Hiyoshi, Kohoku-ku, Yokohama 223-8522, Japan and Institute for Molecular Science, 444-8585 Okazaki, Japan

Kota Daigoku

Computer Center and Department of Chemistry, Tokyo Metropolitan University/ACT-JST, 1-1 Minami-Ohsawa, Hachioji 192-0397, Japan

Morihisa Saeki and Makoto Sakai

Institute for Molecular Science, 444-8585 Okazaki, Japan

Kenro Hashimoto^{a)}

Computer Center and Department of Chemistry, Tokyo Metropolitan University/ACT-JST, 1-1 Minami-Ohsawa, Hachioji 192-0397, Japan

Masaaki Fujii^{b)}

Institute for Molecular Science, 444-8585 Okazaki, Japan

(Received 2 July 2002; accepted 30 July 2002)

The electronic spectra of reaction products via photoexcited phenol/ammonia clusters (1:2–5) have been measured by UV–near-IR–UV ion dip spectroscopy. Compared with the electronic spectra of hydrogenated ammonia cluster radicals the reaction products have been proven to be $(\text{NH}_3)_{n-1}\text{NH}_4$ ($n=2-5$), which are generated by excited-state hydrogen transfer in $\text{PhOH}-(\text{NH}_3)_n$. By comparing the experimental results with *ab initio* molecular orbital calculations at multireference single and double excitation configuration interaction level, it has been found that the reaction products $(\text{NH}_3)_{n-1}\text{NH}_4$ (for $n=3$ and 4), contain some isomers. © 2002 American Institute of Physics. [DOI: 10.1063/1.1508103]

I. INTRODUCTION

Phenol/ammonia and naphthol/ammonia clusters have been investigated as a prototype of excited-state proton transfer (ESPT) for a long time.^{1–16} In the former clusters, however, size-selected electronic transitions were unknown until 1998 because the clusters dissociate after ionization. The peaks of both $\text{PhOH}-(\text{NH}_3)_n^+$ ($n=0,1,\dots$) and $(\text{NH}_3)_{n-1}\text{NH}_4^+$ ($n=1,\dots,5$) appear in a (1+1) resonant enhanced multiphoton ionization (REMPI) mass spectrum of the phenol/ammonia clusters. However, the structured electronic spectrum cannot be obtained when the mass peaks of the parent $\text{PhOH}-(\text{NH}_3)_n^+$ are monitored. In 1998, Kleiner-manns and co-workers found that one can observe the size-selected electronic spectrum if the mass peak of $(\text{NH}_3)_{n-1}\text{NH}_4^+$ is monitored,^{17,18} which raised new questions: Why can the size-selected electronic spectrum be obtained only by monitoring the daughter cations? And how are the daughter cations generated?

Jouvet and co-workers proposed an excited-state hydrogen transfer (ESHT) scenario based on the two-color (1+1') REMPI mass spectrum with a long delay time between two lasers.^{19,20} The ion species, $(\text{NH}_3)_{n-1}\text{NH}_4^+$, are observed even when the ionization laser is delayed by 200 ns

from the excitation laser. This indicates that $(\text{NH}_3)_{n-1}\text{NH}_4^+$ are produced by the ionization of long-lived species generated from $\text{PhOH}-(\text{NH}_3)_n$ in S_1 . No observation of $(\text{NH}_3)_{n-1}\text{NH}_4^+$ by the VUV one-photon ionization mass spectrum has supported this mechanism. From these results, they proposed the interpretation that the long-lived species is a hydrogenated ammonia cluster radical which is generated by a hydrogen transfer reaction



They also suggested that the fast picosecond decay of electronically excited $\text{PhOH}-(\text{NH}_3)_2$ might be due to the dynamics of the hydrogen transfer because ESPT cannot be expected energetically for this cluster.²¹

Hydrogen transfer answers the above questions, and seems to be plausible. However, there was no direct evidence. Recently, we have reported on the vibrational spectra of the reaction products from $\text{PhOH}-(\text{NH}_3)_{3,4}$ using UV–IR–UV ion dip spectroscopy.²² In the present work, we measured the electronic spectra of the reaction products in the near-IR region. The spectra of the products well coincide with those of $(\text{NH}_3)_{n-1}\text{NH}_4$, which were generated from pure ammonia clusters by 193 nm photolysis.^{23,24} From the coincidence, we have proven that the long-lived species are $(\text{NH}_3)_{n-1}\text{NH}_4$. The coexistence of isomers is also discussed based on theoretical calculations.

^{a)}Electronic mail: hashimoto-kenro@c.metro-u.ac.jp

^{b)}Electronic mail: mfujii@ims.ac.jp

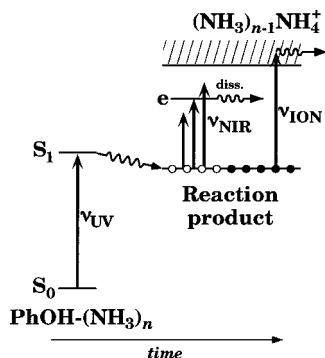


FIG. 1. Principle of the UV-near-IR-UV ion dip spectroscopy.

II. EXPERIMENT

Figure 1 shows the principle of UV-near-IR-UV ion dip spectroscopy to measure the electronic transition of the reaction products from photoexcited $\text{PhOH}-(\text{NH}_3)_n$ in the near-IR region. A pump UV laser (ν_{UV}) was tuned to the S_1-S_0 transition of $\text{PhOH}-(\text{NH}_3)_n$ ($n=2-5$). After a long delay time (180 ns), the near-IR laser (ν_{NIR}) was irradiated and scanned from 4400 to 13 600 cm^{-1} . Then, the ionization laser (ν_{ION}) was irradiated after 20 ns from ν_{NIR} . If ν_{NIR} is resonant to a certain electronic transition, the cluster is pre-dissociated. As a result, the ion signal of $(\text{NH}_3)_{n-1}\text{NH}_4^+$ decreases. The electronic transition of the reaction product which generates $(\text{NH}_3)_{n-1}\text{NH}_4^+$ can be observed as a depletion of the ion signal.

Figure 2 shows the experimental apparatus schemati-

cally. The vapor of phenol at room temperature was seeded in He/ NH_3 (0.5%) or Ne/ NH_3 (0.5%) premix gas (3 bar), and the mixture was expanded into the source chamber (typically 1×10^{-5} Torr) through a pulsed valve (General Valve Series 9). The nozzle diameter was 400 μm . Through a skimmer with a diameter of 2 mm, the molecular beam was introduced to the main chamber (typically 3×10^{-6} Torr), where three lasers ($\nu_{\text{UV}} + \nu_{\text{NIR}} + \nu_{\text{ION}}$) were irradiated. The produced cation was introduced to a linear time-of-flight mass spectrometer (flight path, 1.4 m) and detected by a microsphere plate (EI-Mul C025DTA).

The pump laser ν_{UV} was obtained by a frequency-doubled dye laser (Lumonics HD-500) pumped by the third harmonic of a YAG laser (Spectra Physics GCR-170). The power of ν_{UV} was kept very low to avoid two-photon ionization only by ν_{UV} . The third harmonic of another YAG laser (Lumonics YM1200), or a frequency-doubled dye laser (Continuum ND6000) pumped by the second harmonic of the YAG laser, was used for the ionization laser ν_{ION} (40 μJ). Both UV lasers were combined coaxially by a beam combiner and were focused by a 300 mm focal lens. These YAG lasers, which provided ν_{UV} and ν_{ION} , were operated at 20 Hz. The output of a dye laser (Lumonics HD-500) pumped by the second harmonic of the third YAG laser (Continuum Powerlite 8100) was differentially mixed with 1064 nm in a LiNbO_3 crystal, and was converted to a tunable near-IR laser ν_{NIR} from 4400 to 5500 cm^{-1} . Near-IR laser light from 5500 to 13 600 cm^{-1} was obtained by an OPO laser (Spectra Physics MOPO-HF) pumped by the third harmonic of a YAG

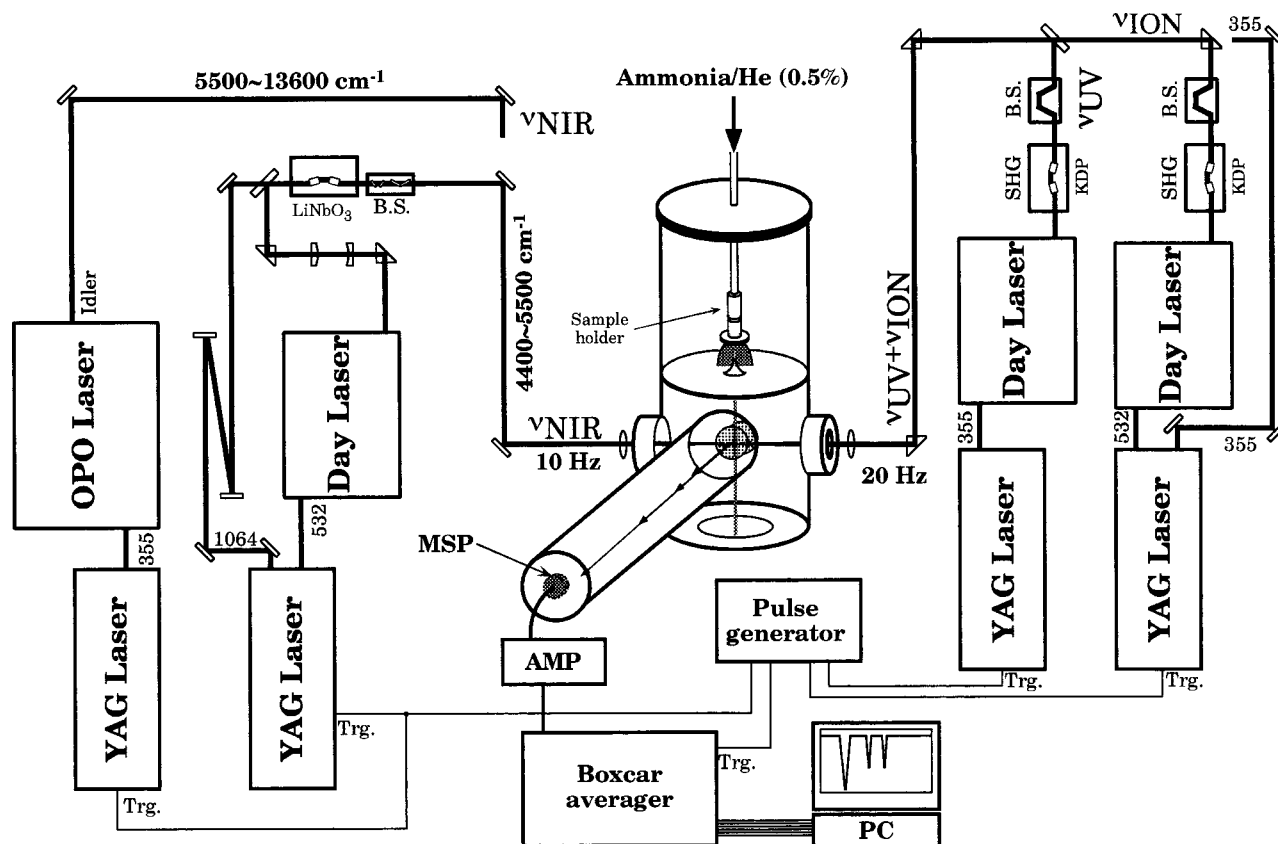


FIG. 2. Schematic diagram of the experimental apparatus.

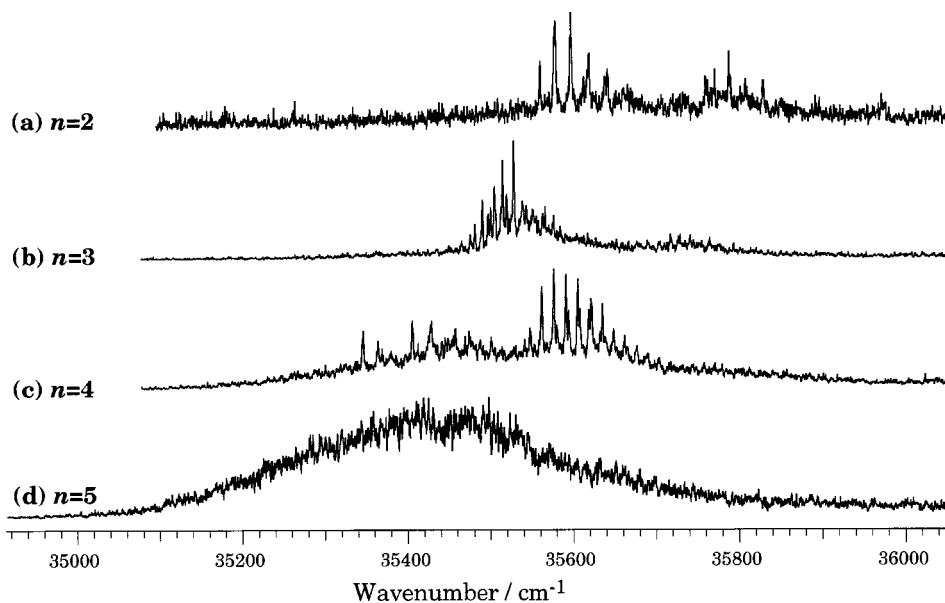


FIG. 3. Long-delayed ($1+1'$) REMPI spectra (action spectra) of $\text{PhOH}-(\text{NH}_3)_n$ obtained by monitoring $(\text{NH}_3)_{n-1}\text{NH}_4^+$. The horizontal axes correspond to wave numbers of the excitation laser ν_{UV} .

laser (Spectra Physics GCR-Pro 250). The near-IR laser was introduced to the main chamber from the opposite side of two UV lasers ($\nu_{\text{UV}} + \nu_{\text{ION}}$), and focused by a CaF_2 300 mm focal lens. The near-IR laser was operated at 10 Hz. The three lasers were synchronized electronically within 1 ns accuracy. We could thus obtain a $\nu_{\text{UV}} + \nu_{\text{NIR}} + \nu_{\text{ION}}$ signal and a $\nu_{\text{UV}} + \nu_{\text{ION}}$ signal alternatively. Each signal was separately integrated and stored in a digital boxcar system (EG&G PARC 4420/4422)²⁵ after amplification by a preamplifier (NF BX31A). The integrated signal was recorded by a personal computer as a function of the NIR laser frequency. By calculating the ratio between the two signals, the fluctuations of the UV laser power and the condition of the pulsed valve were well suppressed. Sample phenol was purchased from Wako Pure Chemical Industries, Ltd. and used after vacuum sublimation.

III. RESULTS AND DISCUSSION

A. Long-delayed ($1+1'$) REMPI spectra of phenol/ammonia (1:2–5) clusters

To determine the wave number of ν_{UV} which excites the phenol/ammonia clusters to S_1 , we measured the long-delayed two-color ($1+1'$) REMPI spectra of $\text{PhOH}-(\text{NH}_3)_n$ ($n=2-5$), i.e., the action spectra of the photochemical reaction of $\text{PhOH}-(\text{NH}_3)_n$. Kleinermanns and co-workers have already reported one-color REMPI spectra of $n=1-4$ clusters.^{17,18} The excitation laser ν_{UV} was irradiated and scanned. After 100 ns from ν_{UV} , the ionization laser ν_{ION} was irradiated. The results are presented in Figs. 3(a)–3(d).

The bands correspond to the vibronic transitions of $\text{PhOH}-(\text{NH}_3)_n$ ($n=2-5$) in the S_1 state. The horizontal axes show the wave number of the excitation laser ν_{UV} . The wavelength of ν_{ION} was fixed to 306.5 nm for $n=2$, and to 355 nm for other sizes. The $n=2$ cluster cannot be ionized by one photon of 355 nm. This supports the expectation that the reaction product might be a hydrogenated ammonia cluster radical whose ionization potential (IP) of NH_3NH_4 is 3.88 eV (~ 320 nm).²⁶ The ionization of the $n=3-5$ clusters by

355 nm light is also consistent with the IP values of $(\text{NH}_3)_{n-1}\text{NH}_4$ ($n=3-5$), being 3.31 eV (~ 375 nm), 2.97 eV (~ 417 nm), and 2.73 eV (~ 454 nm), respectively.²⁶

The spectra in Figs. 3(a)–3(c) show well-resolved low-frequency bands, which are essentially the same as the one-color REMPI spectra by Kleinermanns and co-workers.^{17,18} On the other hand, the electronic spectrum of an $n=5$ cluster [Fig. 3(d)], which is reported for the first time, shows a very broad and unstructured band. This suggests a large geometrical change between S_0 and S_1 , or a vanishing of the reaction barrier, as discussed in a later section.

B. Electronic spectra of the reaction products

Figure 4 shows the electronic spectra of the photochemical reaction products from $\text{PhOH}-(\text{NH}_3)_n$ ($n=2-5$) by UV-near-IR-UV ion dip spectroscopy. The excitation laser ν_1 was fixed to a specific vibronic band in S_1 of $\text{PhOH}-(\text{NH}_3)_n$, which is at 35 544, 35 498, 35 348 cm^{-1} for $n=2-4$, respectively. For $n=5$, ν_{UV} was fixed to the center of the broad peak (282.5 nm). The ν_{ION} for the ionization was 306.5 nm for $\text{PhOH}-(\text{NH}_3)_2$. For $\text{PhOH}-(\text{NH}_3)_n$ of $n=3-5$, the third harmonic of the YAG laser (355 nm) was used as ν_{ION} . The vertical axes of the spectra are proportional to the absorption cross section $\ln[(I_{\text{off}}/I_{\text{on}})/\phi]$, where ϕ is the photon fluence and I_{on} and I_{off} are the signal intensities with and without irradiating ν_{NIR} . This expression of the absorption cross section was also used by Nonose *et al.* for the destruction spectroscopy of $(\text{NH}_3)_{n-1}\text{NH}_4$.^{23,24}

The spectra in Fig. 4 differ remarkably from those of the phenol- $(\text{NH}_3)_n$, but are very similar to the absorption spectra (the photodepletion spectra) of $(\text{NH}_3)_{n-1}\text{NH}_4$ generated from the photolysis of pure ammonia clusters.^{23,24} The electronic transition for the $n=2$ product is observed in a higher region than $\sim 10\,000$ cm^{-1} . The extremely broad bands for the products from $\text{PhOH}-(\text{NH}_3)_{3,4}$ are observed at ≥ 7200 and ≥ 5800 cm^{-1} , respectively, while the band for the $n=5$ product is located at 5000–7200 cm^{-1} being much narrower than those for $n=3$ and 4. All of the spectral feature for n

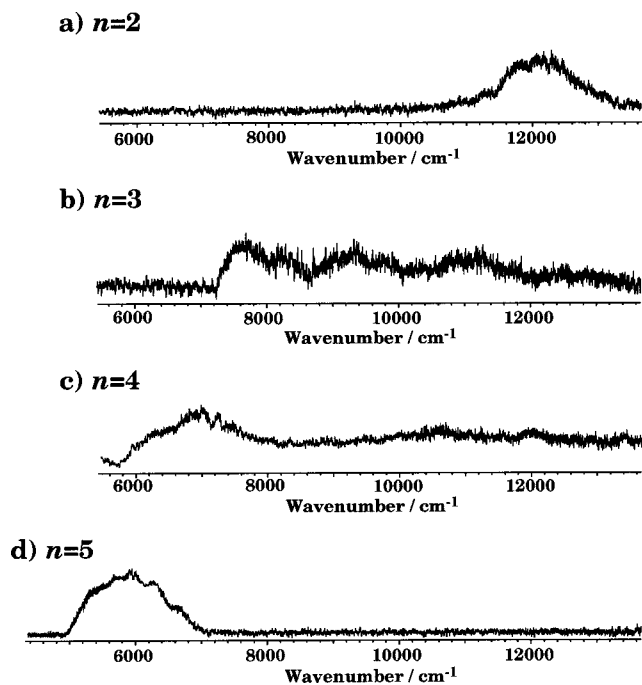


FIG. 4. Electronic spectra of the reaction products from photo-excited $\text{PhOH}-(\text{NH}_3)_n$. The horizontal axes correspond to wave numbers of ν_{NIR} . The vertical axes correspond the absorption cross section by arbitrary units.

$=2-5$ coincide with the electronic spectra of $(\text{NH}_3)_{n-1}\text{NH}_4$ with the same n . Therefore, we concluded that the reaction products from the electronically excited $\text{PhOH}-(\text{NH}_3)_n$ ($n=2-5$) are the hydrogenated ammonia cluster radicals, $(\text{NH}_3)_{n-1}\text{NH}_4$.

Recently, Daigoku *et al.* examined the geometries, vertical transition energies and electronic states of $(\text{NH}_3)_{n-1}\text{NH}_4$ with n up to 4 by *ab initio* MP2 and multireference single and double excitation CI (MRSDCI) methods with the 6-311++G(*d,p*) basis sets augmented by extra diffuse *sp* functions on N atoms.²⁷ According to the calculations, the most stable structures for each n have as many hydrogen bonds as possible between the central NH_4 and the surrounding NH_3 molecules. The incremental binding energies of NH_3 to NH_4 is -6 to -7 kcal/mol with a zero-point vibrational correction (ZPC). Other isomers become less stable as the number of NH_4 - NH_3 hydrogen bonds decreases.

We have extended the calculation to $n=5$ and examined a total of seven plausible isomers at the MP2/6-31++G(*d,p*) level with the Gaussian-98 program.²⁸ The optimized geometries and the total binding energies (TBEs) with and without ZPC are also presented in Fig. 5. All of the structures were confirmed to have real harmonic frequencies; we calculated the harmonic frequencies by numerically differentiating the first derivatives along the nuclear coordinates. The scaled harmonic frequencies were used to include ZPC; the scale factor (0.932) was determined by the average ratio between the experimental fundamental²⁹ and calculated harmonic frequencies of a free NH_3 .

As in the case of $n=4$, **5a** in which NH_4 is surrounded by four NH_3 molecules is the most stable, while those complexes with fewer NH_4 - NH_3 hydrogen bonds are less stable. Thus, we focused on the two most stable structures and re-

fined their relative energies at the same basis sets as in the case of a previous study.²⁷ The results are also shown in Fig. 5. The TBEs for **5a** and **5b** are -26.5 and -24.0 kcal/mol with ZPC, respectively; their deviation is almost the same as the energy difference between the most and the second most stable structures for $n=4$.

The low-lying excited states in $(\text{NH}_3)_{n-1}\text{NH}_4$ are derived from the triply degenerate 1^2T_2 in free NH_4 with T_d symmetry.²⁷ The vertical transition energies (VTEs) to 1^2T_2 -like states in the clusters are mostly determined by the number of NH_3 molecules bound directly to NH_4 . The VTEs for the most stable structure for each n are the lowest among the isomers with the same n , and decrease as n grows by about 1.2 eV from $n=1$ to $n=5$. The band positions of the second most stable structure for n are close to those of the most stable form for $n-1$.

Based on the structure and size dependence of the VTEs, the lowest bands in the electronic spectra of $(\text{NH}_3)_{n-1}\text{NH}_4$ at ~ 1.45 eV ($n=2$), ~ 0.99 – ~ 1.12 eV ($n=3$), ~ 0.81 eV ($n=4$), and ~ 0.72 eV ($n=5$) by destruction spectroscopy were ascribed to $1^2T_2(\text{NH}_4)-1^2A_1(\text{NH}_4)$ -like transitions in the structure, where all NH_3 molecules are bound directly to NH_4 .²⁷ Moreover, the broad band extending to the higher energy region for $n=3$ and 4 was attributed to the same transitions in isomers with fewer NH_4 - NH_3 hydrogen bonds for these sizes. Therefore, the near-perfect coincidence between the previous destruction spectra and the present UV-near-IR-UV ion dip spectra implies that not only the most stable structure, but also the less-stable isomers, were generated by ESHT in $\text{PhOH}-(\text{NH}_3)_{3,4}$ as well as the 193 nm photolysis of ammonia clusters. The remarkable narrowing of the observed band from $n=4$ to $n=5$ may indicate a single product in spite of the similar relative energies between the most and the second most stable isomers for these sizes.

Since nothing was known about the VTEs and oscillator strengths of the high-energy isomer for $n=5$, we computed them for **5a** and **5b** by the MRSDCI method, preceded by complete active space SCF (CASSCF) calculations using the MOLPRO-2000 program package.³⁰ This method is the same as that used previously;²⁷ the results are summarized in Table I. Though the calculations tend to underestimate the absolute VTE values, the transition energies to the 2^2T_2 -like states in **5b** are roughly close to those of the corresponding calculated value of the most stable structure for $n=4$ (0.65 eV). Thus, it seems premature at present to ascribe the remarkable narrowing of the band for $n=5$ to a single isomer. The isomer **5b** may contribute to the higher energy tail of the $n=5$ band extending to ~ 7000 cm^{-1} . Further effort is necessary to argue definitely for the existence of the isomer for $n=5$.

In conclusion, by using UV-near-IR-UV ion dip spectroscopy, we successfully observed the electronic spectra of the reaction products from photoexcited $\text{PhOH}-(\text{NH}_3)_n$ ($n=2-5$). Based on the observed near-IR spectra, we have proven that the reaction products are $(\text{NH}_3)_{n-1}\text{NH}_4$. The radical dissociation of the OH bond occurs in phenol/ammonia clusters despite the acid-base solvated clusters ("forgotten channel"). The reaction products $(\text{NH}_3)_{n-1}\text{NH}_4$

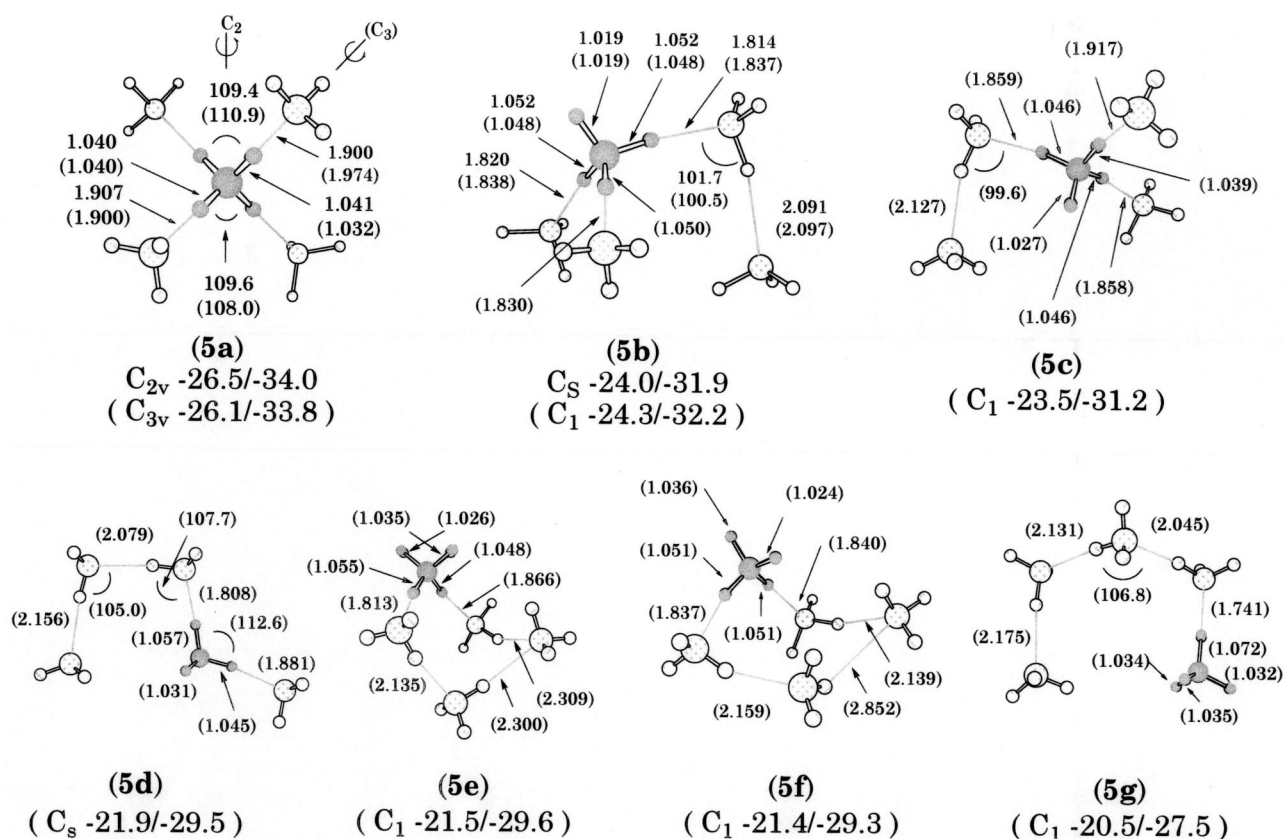


FIG. 5. Optimized structures of $(NH_3)_4NH_4$. Results obtained at the MP2/6-31+G(d,p) level are in parentheses and others were obtained at the 6-311++G(d,p) augmented by diffuse sp functions ($\alpha_{sp}=0.019$) on N atoms (Ref. 27). Geometrical parameters are given in Å and degrees. Molecular symmetry and total binding energies (kcal/mol) with/without ZPC are given under each structure.

(at least for $n=3$ and 4) contain some isomers: The photochemistry of $PhOH-(NH_3)_n$ produces isomers of $(NH_3)_{n-1}NH_4$ for $n=3$ and 4, being similar to the 193 nm photolysis of pure ammonia clusters.

C. Discussion of the reaction mechanism involving ESHT

Recently, Sobolewski and Domcke have studied the ground and the low-lying excited singlet ($^1\pi\pi^*$ and $^1\pi\sigma^*$) states as well as the cationic state ($^2\pi$) of $PhOH-(H_2O)_{1,3}$ and $PhOH-NH_3$ by *ab initio* MO calculations.³¹ They examined the adiabatic potential energy curves (PECs) along the $PhO-H$ stretch coordinate under the C_s symmetry constraint. In bare $PhOH$, S_1 is a bound $^1\pi\pi^*$ state near the ground state equilibrium geometry, while the PEC of S_2 ($^1\pi\sigma^*$) is essentially repulsive along the $O-H$ bond correlating to the

ground state phenoxy radical and hydrogen atom. There exists a conical intersection between the $^1\pi\pi^*$ and $^1\pi\sigma^*$ states, giving rise to the dissociation of the $PhO-H$ bond through the $S_1 \leftarrow S_0$ transition. With the additions of solvent molecules (H_2O and NH_3), electron transfer from the chromophore to the solvent occurs in the $^1\pi\sigma^*$ state. Thus, ESHT is considered to take place through the nonadiabatic transition from $^1\pi\pi^*$ to $^1\pi\sigma^*$, and it is a sequential process of the electron transfer followed by the proton transfer driven by the charge separation.

On the basis of their results, the ESHT is expected to be a tunneling process, which is supported by the experiment of the deuteration for $n=2$ cluster.³² The barrier of the ESHT is determined by the degree of the interaction between the $^1\pi\pi^*$ and $^1\pi\sigma^*$ states. The two-color REMPI spectra of $PhOH-(NH_3)_{2-4}$ show clear vibronic structures, while that of $PhOH-(NH_3)_5$ is structureless (see Fig. 3). This result may suggest that the $PhOH-(NH_3)_5$ has no, or very small, barrier for the ESHT reaction because of the large solvation energy of the $^1\pi\sigma^*$ states.

We have proven the existence of a hydrogen transfer channel in photoexcited phenol/ammonia clusters with the possibility of isomers in the reaction product $(NH_3)_{n-1}NH_4$. It shows that UV-near-IR-UV ion dip spectroscopy is a powerful tool to reveal photochemical reaction products. On the other hand, only by the electronic spectra obtained by UV-near-IR-UV ion dip spectroscopy, it is difficult to discuss the

TABLE I. VTEs (eV) and oscillator strengths (f) corresponding to transitions from ground state to three low-lying excited states for two most stable $(NH_3)_4NH_4$ at the MRSDCI level.

5a ^a			5b		
	VTE	f	VTE	f	
1^2B_1	0.52	0.36	$2^2A'$	0.63	0.36
2^2A_1	0.52	0.36	$1^2A''$	0.66	0.38
1^2B_2	0.52	0.37	$3^2A'$	0.76	0.34

^aReference 27.

reason why the isomers are generated and how the reaction proceeds. Further efforts to unveil the geometries of the reactants and products as well as the potential surfaces are necessary. In order to obtain geometrical information about the reactants and the products, we have examined the vibrational spectra of $\text{PhOH}-(\text{NH}_3)_n$ in S_0 and the reaction products. The preliminary results for $n=3$ and 4 clusters have already been reported in a previous paper.²² The results for other size and with theoretical analysis will be presented in a successive paper. Also a picosecond time-resolved experiment is now in progress to explore the geometrical change taking place with ESHT.³³

ACKNOWLEDGMENTS

This work was supported in part by a Grant-in-Aid from the Ministry of Education, Culture, Sports, Science, and Technology (MEXT) and by the program entitled "Research for the Future" of the Japan Society for the Promotion of Science. A part of the computations was carried out at the Research Center for Computational Science at Okazaki National Research Institutes. The authors thank the Computer Center for the allotment of CPU time. K.H. is grateful for support by Research and Development Applying Advanced Computational Science and Technology, Japan Science and Technology Corporation (ACT-JST).

¹D. Solgadi, C. Jouvét, and A. Tramer, *J. Phys. Chem.* **92**, 3313 (1988).

²C. Jouvét, C. Dedonder-Lardeux, M. Richard-Viard, D. Solgadi, and A. Tramer, *J. Phys. Chem.* **94**, 5041 (1990).

³J. Steadman and J. A. Syage, *J. Chem. Phys.* **92**, 4630 (1990).

⁴J. A. Syage, *J. Soc. Photo-Opt. Instrum. Eng.* **64**, 1209 (1990).

⁵J. Steadman and J. A. Syage, *J. Am. Chem. Soc.* **113**, 6786 (1991).

⁶J. A. Syage and J. Steadman, *J. Chem. Phys.* **95**, 2497 (1991).

⁷J. A. Syage and J. Steadman, *J. Phys. Chem.* **96**, 9606 (1992).

⁸J. A. Syage, *J. Phys. Chem.* **97**, 12523 (1993).

⁹O. Cheshnovsky and S. Leutwyler, *J. Chem. Phys.* **88**, 4127 (1988).

¹⁰J. J. Breen, L. W. Peng, D. M. Willberg, A. Heikal, P. Cong, and A. Zewail, *J. Chem. Phys.* **92**, 805 (1990).

¹¹T. Droz, R. Knochenmuss, and S. Leutwyler, *J. Chem. Phys.* **93**, 4520 (1990).

¹²S. K. Kim, S. Li, and E. R. Bernstein, *J. Chem. Phys.* **95**, 3119 (1991).

¹³E. R. Bernstein, *J. Phys. Chem.* **96**, 10105 (1992).

¹⁴M. F. Hineman, G. A. Brucker, D. F. Kelly, and E. R. Bernstein, *J. Phys. Chem.* **97**, 3341 (1992).

¹⁵M. F. Hineman, D. F. Kelly, and E. R. Bernstein, *J. Chem. Phys.* **99**, 4533 (1993).

¹⁶D. C. Lührs, R. Knochenmuss, and I. Fischer, *Phys. Chem. Chem. Phys.* **2**, 4335 (2000).

¹⁷C. Jacoby, P. Hering, M. Schmitt, W. Roth, and K. Kleinermanns, *Phys. Chem.* **239**, 23 (1998).

¹⁸M. Schmitt, C. Jacoby, M. Gerhards, C. Unterberg, W. Roth, and K. Kleinermanns, *J. Chem. Phys.* **113**, 2995 (2000).

¹⁹G. A. Pino, C. Dedonder-Lardeux, G. Grégoire, C. Jouvét, S. Martrenchard, and D. Solgadi, *J. Chem. Phys.* **111**, 10747 (1999).

²⁰G. A. Pino, G. Grégoire, C. Dedonder-Lardeux, C. Jouvét, S. Martrenchard, and D. Solgadi, *Phys. Chem. Chem. Phys.* **2**, 893 (2000).

²¹G. Grégoire, C. Dedonder-Lardeux, C. Jouvét, S. Martrenchard, A. Pere-mans, and D. Solgadi, *J. Phys. Chem. A* **104**, 9087 (2000).

²²S. Ishiuchi, M. Sasaki, M. Sakai, and M. Fujii, *Chem. Phys. Lett.* **322**, 27 (2000).

²³S. Nonose, T. Taguchi, K. Mizuma, and K. Fuke, *Eur. Phys. J. D* **9**, 309 (1999).

²⁴S. Nonose, T. Taguchi, F. Chen, S. Iwata, and K. Fuke, *J. Phys. Chem. A* **106**, 5242 (2002).

²⁵Y. Okuzawa, M. Fujii, and M. Ito, *Chem. Phys. Lett.* **171**, 341 (1990).

²⁶K. Fuke, R. Takasu, and F. Misaizu, *Chem. Phys. Lett.* **229**, 597 (1994).

²⁷K. Daigoku, N. Miura, and K. Hashimoto, *Chem. Phys. Lett.* **346**, 81 (2001).

²⁸M. J. Frisch, G. W. Trucks, H. B. Schlegel *et al.* GAUSSIAN 98, Revision A.9, Gaussian, Inc., Pittsburgh, PA, 1998.

²⁹G. Herzberg, *Molecular Spectra and Molecular Structure* (Van Nostrand Reinhold, New York, 1945), Vol. II.

³⁰MOLPRO is a package of *ab initio* programs written by H. J. Werner and P. J. Knowles, with contributions of J. Almlof, R. D. Amos, M. J. O. Deegan *et al.*

³¹A. L. Sobolewski and W. Domcke, *J. Phys. Chem. A* **105**, 9275 (2001).

³²G. Grégoire, C. Dedonder-Lardeux, C. Jouvét, S. Martrenchard, and D. Solgadi, *J. Phys. Chem. A* **105**, 5971 (2001).

³³S. Ishiuchi, M. Sakai, K. Daigoku, T. Ueda, T. Yamanaka, K. Hashimoto, and M. Fujii, *Chem. Phys. Lett.* **347**, 87 (2001).